

IFUSP/P 338

B.I.F. - USP

UNIVERSIDADE DE SÃO PAULO

INSTITUTO DE FÍSICA
CAIXA POSTAL 20516
01000 - SÃO PAULO - SP
BRASIL

publicações

IFUSP/P-338

THE EFFECT OF THE TWO-STEP α TRANSFER
REACTION IN THE ELASTIC SCATTERING OF
 $^{12}\text{C} + ^{24}\text{Mg}$

by

R.Lichtenthaler F ϕ , A.Lépine-Szily,
A.C.C.Villari, W.Mittig, V.J.G.Porto
and C.V.Acquadro

B.I.F. - USP

Instituto de Física - U. S. P.

THE EFFECT OF THE TWO-STEP α TRANSFER REACTION IN THE ELASTIC
SCATTERING OF $^{12}\text{C} + ^{24}\text{Mg}$

R. Lichtenthaler Fº, A. Lépine-Szily, A. C. C. Villari, W. Mittig,
V.J.G. Porto and C.V. Acquadro
Instituto de Física, Universidade de São Paulo, Caixa Postal 20516
São Paulo, Brasil

A B S T R A C T

Angular distribution of the elastic scattering $^{24}\text{Mg}(^{12}\text{C}, ^{12}\text{C})^{24}\text{Mg}$ and of the $^{24}\text{Mg}(^{12}\text{C}, ^{16}\text{O})^{20}\text{Ne}$ transfer reaction have been measured at 40 MeV incident energy, respectively in the $20^\circ \leq \theta_{\text{CM}} \leq 115^\circ$ and $20^\circ \leq \theta_{\text{CM}} \leq 60^\circ$ angular regions.

The elastic scattering and transfer reactions were analysed with Frahn's closed formalism as well as with optical model calculations. The influence of the two-step α -transfer channel ($^{12}\text{C} + ^{24}\text{Mg} \rightarrow ^{16}\text{O} + ^{20}\text{Ne} \rightarrow ^{12}\text{C} + ^{24}\text{Mg}$) on the elastic scattering was calculated explicitly using the coupled channel extension of the closed formalism. This calculation shows that the coupling between the α -transfer and elastic channel can account for the intermediate angle oscillations observed in the elastic scattering angular distributions.

JUN/1982

I. INTRODUCTION

A great amount of experimental data was collected since the first observation⁽¹⁾ of unexpectedly large cross-sections near $\theta_{\text{CM}}=180^\circ$ for the elastic and inelastic scattering of $^{16}\text{O} + ^{28}\text{Si}$ at $E_{\text{CM}}=35$ MeV. Elastic and inelastic scattering excitation function measurements at 180° for $^{16}\text{O} + ^{28}\text{Si}$ ⁽²⁾, $^{12}\text{C} + ^{28}\text{Si}$ ⁽²⁾, $^{12}\text{C} + ^{24}\text{Mg}$ ⁽³⁾ exhibit strong and regular structures with width of about 1-2 MeV and large peak-to-valley ratio. Similar structures have been seen in the forward⁽⁴⁾ as well as backward-angle⁽⁵⁾ excitation functions of the α -transfer reaction $^{24}\text{Mg}(^{16}\text{O}, ^{12}\text{C})^{28}\text{Si}$ and in the backward angle excitation function⁽⁶⁾ of the reaction $^{28}\text{Si}(^{16}\text{O}, ^{12}\text{C})^{32}\text{S}$ and in the forward angle excitation function of the reaction $^{20}\text{Ne}(^{16}\text{O}, ^{12}\text{C})^{24}\text{Mg}$ ⁽²⁸⁾.

Angular distributions of the elastic scattering of $^{16}\text{O} + ^{28}\text{Si}$ ⁽⁷⁾, $^{12}\text{C} + ^{28}\text{Si}$ ^(8,9), $^{12}\text{C} + ^{24}\text{Mg}$ ⁽¹⁰⁾ and $^{16}\text{O} + ^{24}\text{Mg}$ ⁽¹²⁾, as well as the above mentioned α -transfer reactions^(6,11), exhibit strong oscillatory patterns and a rise of some orders of magnitude in the cross-section at $\theta_{\text{CM}}=180^\circ$.

The entrance and exit channel elastic scattering excitation functions, corresponding to the α -transfer reactions $^{24}\text{Mg}(^{16}\text{O}, ^{12}\text{C})^{28}\text{Si}$ and $^{28}\text{Si}(^{16}\text{O}, ^{12}\text{C})^{32}\text{S}$, have also been measured at $\theta_{\text{CM}}=180^\circ$ and there seems to be no clear correlation between the structures in different channels or at different angles.

It has been observed that these phenomena are most significant when the target and projectile have $n \times \alpha$ structure and the addition of one or a few nucleons^(9,13,14) to the target or projectile reduces greatly or eliminates the observed effects. Recent data⁽⁷⁾ on the elastic scattering of ^{16}O on ^{29}Si and ^{30}Si constitute an exception to the above rule, the backward angle excitation function exhibiting regular structures of the same width as $^{16}\text{O} + ^{28}\text{Si}$, with a moderate reduction (from factor 5 for

^{29}Si , to factor 50 for ^{30}Si) in the 180° cross-section. The physical origin of these phenomena is not fully understood yet. However, several explanations have been proposed, ranging from surface-transparent⁽¹⁵⁾ and parity dependent^(16,17) optical potentials, S-matrix descriptions including explicitly the interference⁽⁷⁾ between the barrier wave and the internal wave, introducing an ℓ -window in the S-matrix⁽¹⁸⁾ or isolated resonances^(7,11) in the composite system superposed to direct reaction background.

There is a clear indication that the over-all picture one obtains may be summarized as follows^(18,19): the elastic scattering amplitude of these α -nuclei is composed of three terms; an "E-18"-type contribution arising from the global "optical" properties of the interacting pair, which is common to all heavy-ion systems, a parity-independent anomalous window and finally a parity-dependent window that contributes mostly in the back-angle region.

It was clearly shown in Ref.18 that such a picture reproduces rather well both the 180° excitation function and the full angular distribution. Similar interpretation was invoked in Ref. 20 in connection with the 90° excitation function.

A possible mechanism that may give rise to these anomalous windows, which was suggested in Ref. 18 and 19, is based on a multistep α -transfer contribution to the elastic amplitude. These authors relate the parity-independent anomalous window to the polarization in the elastic channel due to its coupling to a single- α transfer channel. The parity-dependent window, which was found to be much smaller in magnitude is then related to a higher-order process involving the elastic transfer of three α -particles.

In order to test this hypothesis one would necessarily have to deal with a complicated multi-coupled channel description.

One may, though, simplify the description by exploiting

the fact that the contribution to the elastic amplitude arising from the parity-dependent window is concentrated mostly in the back-angle region. Therefore one should be able to test the dynamical origin of the parity-independent window, referred to above, by analysing the angular distribution in the intermediate angle region.

For this reason we measured the angular distributions of the elastic scattering $^{24}\text{Mg}(^{12}\text{C},^{12}\text{C})^{24}\text{Mg}$ in the forward and intermediate angle region and the α -transfer reaction $^{24}\text{Mg}(^{12}\text{C},^{16}\text{O})^{20}\text{Ne}$ in the forward angle region at 40 MeV incident energy. The calculation which includes the effect of the two-step α -transfer on the elastic scattering was performed in the frame of Frahn's closed formalism⁽²¹⁾, and it shows that the coupling can account for the intermediate angle oscillations observed in the elastic scattering angular distribution.

II. EXPERIMENTAL METHOD AND RESULTS

The angular distributions of the reactions $^{24}\text{Mg}(^{12}\text{C},^{12}\text{C})^{24}\text{Mg}$ and $^{24}\text{Mg}(^{12}\text{C},^{16}\text{O})^{20}\text{Ne}$ were measured using a ^{12}C beam accelerated to 40 MeV by the São Paulo Pelletron Accelerator. Targets of isotopically enriched ^{24}Mg , evaporated in ^{12}C backing were used. Three sets of ΔE -E telescopes were used, the E detectors being standard Si surface barrier detectors and the ΔE detectors proportional counters for the forward angles and surface barrier detectors for the backward angle data. At backward angles the ^{16}O provenient from the transfer reaction were stopped in the ΔE detectors. The reason for the use of telescopes was the necessity of identification for the transfer reaction at forward angles, and the presence of light particles, provenient from the fusion of $^{12}\text{C} + ^{12}\text{C}$ and $^{12}\text{C} + ^{16}\text{O}$, at backward angles. For normalization

purposes a $1 \mu\text{g}/\text{cm}^2$ thick gold layer was evaporated on the targets. A monitor detector placed at 15° with respect to the beam permitted to calculate the ratio of ^{24}Mg to gold target thicknesses. The absolute cross sections were obtained by normalizing to Rutherford scattering on gold and using the ratio of target thicknesses. The energy resolution at all angles was sufficient to separate the elastic peak from inelastic peaks.

At some angles the ^{16}O ions recoiling elastically from the target have the same energy as the ^{16}O ions provenient from the α -transfer reaction. The thickness of the ^{16}O layer in target was determined by two independent methods: the elastic scattering of ^{12}C on ^{16}O was measured from $\theta_{\text{LAB}}=20^\circ$ to 30° at $E_{\text{LAB}}=24$ MeV and compared to absolute cross-sections measured by Kuehner et al. (22) and the 40 MeV elastic scattering of ^{12}C on ^{16}O was compared to absolute cross-sections measured by Charles et al. (23). These two methods yielded target thicknesses which were within 10% in accord. The recoil cross section was obtained for all measured angles from the complete elastic scattering angular distribution measured by Charles (23). These recoil counts were subtracted from the total counts at all angles where the kinematic overlap of peak energies was verified. This procedure introduced an additional error in the measured transfer cross-sections.

The typical spectrum of ^{12}C ions elastically scattered to 40° , is presented in figure 1. The spectra of ^{16}O ions provenient from the transfer reaction and from the recoil are shown in figure 2. The angular distributions of elastic scattering and transfer reactions are presented respectively in figures 3 and 4. The absolute errors in the elastic cross-sections are 5% for the forward angles and 10%-20% for intermediate angles. The elastic angular distribution presents pronounced oscillations at intermediate angles, which are characteristics of the α -structure nuclei in this energy region.

The period of oscillations is $\sim 10^\circ$ in accord with the prevision obtainable from the grazing angular momentum $l_g=18$. The transfer angular distribution is also oscillatory and the period is the same as in the elastic scattering, depicting the contribution of grazing surface partial waves to the transfer cross-section.

III. ANALYSIS OF THE DATA

III.A) Frahn - Hussein's formalism

In a recent work Frahn and Hussein (21) developed an extension of the closed formalism for elastic heavy-ion collisions to account for channel coupling effects on this process. The specific transfer channel that will be taken into account is the double α -transfer presented schematically in figure 5.

The contribution of other transfer channels, involving the excited states of ^{20}Ne or other intermediate systems as $^8\text{Be} + ^{12}\text{C}$ e.g., could also be taken into account in a straight-forward way.

The procedure (21) starts from the set of coupled-channels equations and using the radial Gellmann-Goldberger relation writes the total nuclear S-matrix as the sum of the uncoupled elastic S-matrix and a correction term that describes the coupling to the α -transfer channel. The use of the on-shell approximation which was invoked in Ref. 21, implies that the intermediate system is taken out to infinity and is brought back again

$$S_{\ell_n}^N(k_n) = S_{\ell_n}^N(k_n) + S_{\ell_n}^N(k_n) = S_{\ell_n}^N(k_n) \left[1 - t_{\ell_n}(k_n k_m) \right] \quad (1)$$

where t_{ℓ_n} is written in terms of DWBA radial integrals $R_{\ell_n \ell_m}$ and

$$R_{\ell_m \ell_n}^{L} = \frac{\mu_n^2 k_n k_m}{2\pi^2 \hbar^4} a_{\ell_m \ell_n} a_{\ell_n \ell_m} \frac{R_{\ell_n \ell_m}(k_n k_m) R_{\ell_m \ell_n}(k_m k_n)}{\tilde{S}_{\ell_n}^N(k_n) \tilde{S}_{\ell_m}^N(k_m)} \quad (2)$$

where $a_{\ell_n \ell_m}$ is the strength of the coupling interaction

$$V_{\ell_n \ell_m}^{L}(r) = a_{\ell_n \ell_m} F(r) \equiv a_T(k_n k_m) F(r) \quad (3)$$

and contains the spectroscopic factors and geometric factors. The DWBA radial integrals are factorized in terms of coulomb radial integrals and the unperturbed nuclear S-matrix, using the Sopkovitch approximation⁽²⁴⁾

$$R_{\ell_n \ell_m}^L(k_n k_m) = \frac{2\pi}{\epsilon_n k_n k_m K_n} \left[\tilde{S}_{\ell_n}^N(k_n) \right]^{1/2} I_{L-K}(\theta, \xi) \left[\tilde{S}_{\ell_m}^N(k_m) \right]^{1/2} \quad (4)$$

the coulomb radial integrals I_{L-K} are calculated in the WKB approximation⁽²⁴⁾. Supposing that the channel spin $I_n = I_m = 0$, $L=0$, $K=0$ and the total S-matrix can be written as a continuous function of the variable $\lambda = \ell + \frac{1}{2}$ as

$$\tilde{S}^N(\lambda) = \tilde{S}(\lambda) [1 - t(\lambda)] = \tilde{S}(\lambda) \left[1 - \frac{2\mu^2}{\hbar^4} \frac{a_T(K_n K_m) a_T(k_m k_n) I_{00}^{(K_n)} I_{00}^{(K_m)}}{\epsilon_n k_n k_m \epsilon_m k_m k_m} \right] \quad (5)$$

K_n, K_m are the imaginary wave numbers of the bound states n and m , k_n, k_m are wave numbers in the channels n and m and ϵ_n, ϵ_m are scale factors that partly account for recoil effects. The profile of the correction term in the S-matrix is bell-shaped and centered around $\Lambda_T = \Lambda + \delta_T$, where δ_T is determined by characteristics of the unperturbed nuclear S-matrix and by the wave numbers and Sommerfeld parameters of the channels n and m .

We note that the contribution to the elastic S-matrix due to transfer channel coupling is completely determined by the characteristics of the transfer process. The elastic scattering amplitude can be calculated from the S-matrix by the sum of partial waves.

$$f(\theta) = \frac{i}{k} \sum_{\ell} \left(\ell + \frac{1}{2} \right) [1 - S_{\ell}(k)] P_{\ell}(\cos \theta) \quad (6)$$

The scattering amplitude also can be written as a sum of two terms:

$$f(\theta) = \hat{f}(\theta) + \tilde{f}(\theta) \quad (7)$$

$$\text{where } \hat{f}(\theta) = \frac{i}{k} \sum_{\ell} \left(\ell + \frac{1}{2} \right) [1 - \hat{S}_{\ell}(k)] P_{\ell}(\cos \theta) \quad (8)$$

$$\text{and } \tilde{f}(\theta) = - \frac{i}{k} \sum_{\ell} \left(\ell + \frac{1}{2} \right) \tilde{S}_{\ell}(k) P_{\ell}(\cos \theta) \quad (9)$$

Analytic expressions for $\hat{f}(\theta)$ representing the leading terms in an asymptotic expansion for large Sommerfeld parameters and large grazing angular momenta have been derived by Frahn⁽²⁵⁾. Similar methods are used to evaluate the amplitude $\tilde{f}(\theta)$ ⁽²¹⁾

The analytic expression derived for $\tilde{f}(\theta)$ and valid in the angular range $\frac{1}{\Lambda_T} \leq \theta \leq \pi$ is

$$\tilde{f}(\theta) = \frac{i\Lambda_T}{2k_n} e^{2i\sigma(\Lambda_T)} \left(\frac{\pi - \theta}{\sin \theta} \right)^{1/2} t(\Lambda_T) \left\{ H_T^+(\theta) \left[J_0(\Lambda_T(\pi - \theta)) + iJ_1(\Lambda_T(\pi - \theta)) \right] \right. \\ \left. + H_T^-(\theta) \left[J_0(\Lambda_T(\pi - \theta)) - iJ_1(\Lambda_T(\pi - \theta)) \right] \right\} \quad (10)$$

where $J_0(x)$ and $J_1(x)$ are cylindrical Bessel functions, $H_T^{\pm}(\theta)$ are functions depending on the particular parameterization used for the unperturbed S-matrix, the normalization of the amplitude $\tilde{f}(\theta)$ is contained in the term $t(\Lambda_T)$:

$$t(\Lambda_T) = \frac{1}{2} \frac{\mu_n \mu_m}{\hbar^4 k_n k_m^*} a_T(k_n k_m) a_T(k_m k_n) I_{00}^{(k_n)}(\theta_R^+ \xi) I_{00}^{(k_m)}(\theta_R^+ \xi) \quad (11)$$

$$a_T(k_n k_m) = N_1 N_2 (-1)^{\ell_1} \frac{\hbar^2}{2\mu_T} k_n^{-\ell_1} k_m^{\ell_1-1} \quad (12)$$

where $N_1 N_2$ is the product of the spectroscopic factors of the target and projectile and ℓ_1 is the orbital angular momentum of the transferred α particle in ^{24}Mg .

III.B) Numerical results

In order to calculate the elastic cross-section

$$\left(\frac{d\sigma}{d\Omega}\right)_{\text{elastic}} = |\tilde{f}(\theta) + \bar{\tilde{f}}(\theta)|^2 \quad (13)$$

taking into account the influence of the double α transfer on the elastic channel, we have to calculate $\tilde{f}(\theta)$ and $\bar{\tilde{f}}(\theta)$.

III.B.a) Unperturbed amplitude $\tilde{f}(\theta)$

In order to calculate the unperturbed amplitude $\tilde{f}(\theta)$ we need the unperturbed S-matrix $\hat{S}(\lambda)$ which describes the interaction of $^{12}\text{C} + ^{24}\text{Mg}$ at 40 MeV. As we claim that the intermediate and backward angle oscillations are due to the double α -transfer channel, we determinate $\hat{S}(\lambda)$ from an optical potential that fits all forward angle elastic scattering data of $^{12}\text{C} + ^{24}\text{Mg}$ at energies from $E_{\text{LAB}} = 19\text{MeV}$ to 40 MeV. Unpublished data from São Paulo⁽²⁶⁾ at $E_{\text{LAB}} = 19, 21, 23\text{MeV}$, data at $E_{\text{LAB}} = 24.8, 31.20, 34.80\text{ MeV}$ from Mermaz⁽¹⁰⁾ data at $E_{\text{LAB}} = 21$ and 24 MeV from Carter⁽²⁷⁾ were analyzed together with our 40MeV data. Two potentials were successful in fitting the forward angle region at all energies; they are presented on table I. The real and imaginary potentials have the usual Woods-Saxon form

and the radii are defined as $R_{R,I} = r_{R,I} (A_T^{1/3} + A_P^{1/3})$ and $R_C = r_C (A_T^{1/3} + A_P^{1/3})$. The potential X3 is derived from E18 just changing the imaginary radius and diffuseness and potential I was obtained by Kono and Mittig⁽²⁶⁾ for the lower energy data. Carter's potential⁽²⁷⁾ was not adequate for other energies.

The fits obtained with these two potentials are shown in figures 6 and 7. The reflection functions n_ℓ calculated from these two potentials are presented in figure 8. In our closed formalism calculations we used the Ericson's parametrization for the unperturbed S-matrix:

$$\hat{S}(\lambda) = \frac{1}{1 + \exp\left(\frac{\Lambda - \lambda}{\Delta} - i\alpha\right)} \quad (14)$$

The $\hat{S}(\lambda)$ adopted in our calculation has a reflection function $|\hat{S}(\lambda)|$ which reproduces well the optical potential reflection functions, it is represented by the dot-dashed curve in figure 8.

The parameters Λ, Δ and α are found to be

$$\Lambda = 18.7 \quad \Delta = 1.3 \quad \alpha = 0.5$$

The fit obtained to the elastic scattering data at 40MeV from $\frac{d\sigma}{d\Omega} = |\tilde{f}(\theta)|^2$ using these parameters in $\hat{S}(\lambda)$ and calculating $\tilde{f}(\theta)$ by the explicit summation of partial waves is presented in figure 9 as the dashed line. It reproduces well the forward angle data, but deviates from data at intermediate angles and presents no oscillations there.

III.B.b) The amplitude $\tilde{f}(\theta)$

As we have seen before, the amplitude $\tilde{f}(\theta)$ depends only on the characteristics of the transfer process. In order to determine the relevant characteristics of the α -transfer

$^{12}\text{C} + ^{24}\text{Mg} \rightarrow ^{16}\text{O} + ^{20}\text{Ne}$ we analyzed these transfer data in the frame of Frahn's closed formalism for transfer⁽²⁴⁾. Beginning with the DWBA transition amplitude and using the approximations already mentioned before, one obtains, for $L=0$ $K=0$ $M=0$

$$\left(\frac{d\sigma}{d\Omega}\right)_{\text{transfer}} = |f_T(\theta)|^2 = \frac{A_{n,m}^{\mu_n \mu_m}}{(2\pi\hbar^2)^2} \frac{k_n}{k_m} \frac{\pi}{(k_n k_m K)^2} \frac{\theta}{\sin\theta} \left| (d_{00}^0)^2 A_T \right. \\ \left. I_{00}^K(\theta_R^T, \xi) e^{\gamma\delta_T} e^{i2\delta_k(\Lambda_T)} \pi A \left\{ H^+(\theta) \left[J_0(\Lambda_T\theta) + iJ_1(\Lambda_T\theta) \right] + \right. \right. \\ \left. \left. + H^-(\theta) \left[J_0(\Lambda_T\theta) - iJ_1(\Lambda_T\theta) \right] \right\} \right|^2 \quad (15)$$

In the actual calculation of $f_T(\theta)$ we used an asymptotic expansion for the cylindrical Bessel functions J_0 and J_1 valid in forward and intermediate angles. The quantity A , which is a normalization factor, related to the strength of the interaction $V_{n,m}$ responsible for the $n \rightarrow m$ transfer, contains the spectroscopic factor, geometric and spin factors. The derivation of $f_T(\theta)$ is based on zero range and no-recoil assumptions. We know that these dynamic effects are important and the absolute transfer cross-section calculated without taking into account these dynamic effects can be underestimated by orders of magnitude. For practical purposes we define the normalization factor $A = \frac{(\frac{d\sigma}{d\Omega})_{\text{exp}}}{(\frac{d\sigma}{d\Omega})_{\text{theor}}}$ and it will contain the usual geometric, spectroscopic and spin factors together with a dynamic factor determined empirically.

The comparison of the experimental transfer cross-section and the theoretical calculations, which gives a good fit to the data using the above formula, permits to obtain the relevant parameters of the transfer amplitude

$$A_T = 18.27 \quad \Delta_T = 0.3 \quad \alpha_T = 1.57$$

The results of the above transfer calculation are presented in figure 10.

If we compare the expressions of the double α transfer amplitude $\bar{f}(\theta)$ and the single α transfer amplitude $f_T(\theta)$, we can verify that they have the same angular dependence and that $\bar{f}(\theta)$ is proportional to the square of $f_T(\theta)$ showing in a certain manner that $\bar{f}(\theta)$ describes the round-trip of an α particle from ^{24}Mg to ^{12}C and back again. The normalization of $\bar{f}(\theta)$ is known except for the empirical dynamic factor due to the zero range and no-recoil nature of the calculation. The way we introduce this dynamic factor into $\bar{f}(\theta)$ is to assume that the strength $a_T(K_n K_m)$ of the coupling interaction is the same both in the derivation of $f_T(\theta)$ and that of $\bar{f}(\theta)$. This assumption leads to the following relation between the normalization factors

$$N^2 = N_1 N_2 = \frac{2\mu_T}{\xi\hbar} \left(\frac{2J_i+1}{2J_f+1} \cdot A \cdot K_n K_m \right)^{\frac{1}{2}} \quad (16)$$

The normalization factor obtained from A , empirically determined by adjusting the transfer cross section, is $N=1300$.

The complete calculation, adding to the elastic amplitude $f(\theta)$ the amplitude $\bar{f}(\theta)$, calculated with the parameters $\Lambda_T, \Delta_T, \alpha_T$ and N conveniently determined from the transfer reaction gives an angular distribution where the amplitudes of oscillations are of the same order of magnitude as the experimental ones, the period is also correct, but the oscillations are somewhat out of phase. We performed calculations introducing an arbitrary phase ϕ between $f(\theta)$ and $\bar{f}(\theta)$

$$\left(\frac{d\sigma}{d\Omega}\right)_{\text{elastic}} = |f(\theta) + e^{i\phi} \bar{f}(\theta)|^2 \quad (17)$$

and determined $\phi = 2.0$ rd.

The result of the calculation with phase ϕ is presented in the figure 9, as the continuous line. It reproduces well the forward angle and intermediate angle oscillations.

One possible origin of ϕ may be traced to the off-shell effects, which were completely neglected in Ref. 21.

IV. CONCLUSIONS

The aim of this study was to test the hypothesis that the oscillations seen in the angular distributions at intermediate angles are related to the polarization in the elastic channel due to its coupling to a single- α transfer channel. Using the picture discussed in section III we found a good accord with the data; the period and amplitude of oscillations being comparable at intermediate angles. The only adjusted parameter to fit the elastic data is the relative phase between the amplitudes $\hat{f}(\theta)$ and $\tilde{f}(\theta)$. The other parameters were fixed by the transfer data or by a large amount of elastic data at other energies.

From our calculations we can conclude that the channel coupling to α -transfer process could have an important effect at intermediate angles and at energies above the coulomb barrier. At backward angles, the elastic transfer, which produces a parity dependent term in the nuclear S-matrix should come into play. As the spectroscopic factor for the elastic transfer of a ^{12}C must be very small, the successive transfer of three α -particles can be also responsible for the very backward rise in the cross-section.

The main advantage of doing the kind of calculation reported here within the framework of the closed formalism is the mathematical simplicity, which permits to have a better physical insight into the processus.

ACKNOWLEDGEMENTS

We would like to thank Prof. M. S. Hussein for very fruitful discussions, and the late Prof. W.E. Frahn for a most rewarding collaboration that we had with him during two visits that he made to our Institute. The financial support of FAPESP and CNPq is acknowledged.

REFERENCES

- 1) P.Braun-Munzinger, G.M.Berkowitz, T.M.Cormier, J.W.Harris, C.M. Jachcinski, J.Barrette and M.J.Levine - Phys.Rev.Lett. 38, 944 (1977).
- 2) J.Barrette, M.J.Levine, P.Braun-Munzinger, G.M.Berkowitz, M. Gai, J.W.Harris and C.M.Jachcinski - Phys.Rev.Lett. 40, 445 (1978).
- 3) A.Greiner, B.T.Kim, N.Lisbona, M.C.Mermaz, M.Petrascu, M. Petrovici and V.Simion - Comptes Rendu d'Activité de CEN Saclay 1978-1979 and preprints.
- 4) M.Paul, S.J.Sanders, J.Cseh, P.F.Geesaman, W.Henning, D.G.Kovar, C.Olmer and J.P.Schiffer - Phys.Rev.Lett. 40, 1310 (1978).
- 5) S.M.Lee, J.C.Adloff, P.Chevalier, D.Disdier, V.Rauch and F. Scheibling - Phys.Rev.Lett. 42, 429 (1979).
- 6) G.K.Gelbke, T.Awes, U.E.P.Berg, J.Barrette, M.J.Levine, P.Braun-Munzinger - Phys.Rev.Lett. 41, 1778 (1978).
- 7) P.Braun-Munzinger, G.M.Berkowitz, M.Gai, G.M.Jachcinski, T.R. Renner, C.D.Uhlhorn, J.Barrette and M.J.Levine - Phys.Rev. C24, 1010 (1981).
- 8) M.R.Clover, R.M.Devries, R.Ost, N.J.A.Rust, R.N.Cherry Jr., H. E.Gove - Phys.Rev.Lett. 40, 1008 (1978).
- 9) R.Ost, M.R.Clover, R.M.Devries, B.R.Fulton, H.E.Gove and N.J. Rust - Phys.Rev. C19, 740 (1979).
- 10) M.C.Mermaz, A.Greiner, B.T.Kim, M.Levine, E.Muller and M.Ruscev - XXI International Winter Meeting on Nuclear Physics, Bormio, 1981.
- 11) S.J.Sanders, M.Paul, J.Cseh, D.F. Geesaman, W.Henning, D.G. Kovar, R.Kozub, C.Olmer and J.P.Schiffer - Phys.Rev. C21, 1810 (1980).
- 12) M.Paul, S.J.Sanders, D.F.Geesaman, W.Henning, D.G.Kovar, C.Olmer, J.P.Schiffer, J.Barrette and M.J.Levine - Phys.Rev. C21, 1802 (1980).

- 13) J.C.Peng, D.L.Hanson, J.D.Moses, D.W.B.Schult, N.Stein, J.W. Sunier and N.Cindro - Phys.Rev.Lett. 42, 1458 (1979).
- 14) P.Braun-Munzinger and J.Barrette in Proceedings of Symp. on Heavy-Ion Elastic Scattering, Rochester 1977 p.85.
- 15) S.Kahana, B.T.Kim, M.C.Mermaz - Phys.Rev. C20, 2124 (1979).
- 16) D.Dehnhard, V.Shkolnik, M.A.Franey - Phys.Rev.Lett. 40, 1549 (1978).
- 17) S.Kubono, P.D.Bond, D.Horn, C.E.Thorn - Phys.Lett. 84B, 408 (1979).
- 18) W.E.Frahn, M.S.Hussein, L.F.Canto and R.Donangelo - Nucl.Phys. A369, 166 (1981).
- 19) J.Barrette and S.Kahana, Comment Nucl.Part.Phys. 9, 67 (1980).
- 20) M.S.Hussein and M.P.Pato - Phys.Rev. 25C, 1895 (1982).
- 21) W.E.Frahn, M.S.Hussein - Nucl.Phys. A346, 237 (1980).
- 22) J.A.Kuehner, E.Almquist and D.A.Bromley - Phys.Rev. 131, 1254 (1963).
- 23) P.Charles, F.Auger, I.Badawy, B.Berthier, M.Dost, J.Gastebois, B.Fernandez, S.M.Lee, E.Plagnol, Comptes Rendu d'activité CEN Saclay 1975-1976.
- 24) W.E.Frahn - Phys.Rev. C21, 1870 (1980).
- 25) W.E.Frahn, D.H.E.Gross - Ann. of Phys. 101, 520 (1976).
- 26) Y.Kono and W.Mittig, unpublished.
- 27) J.Carter, R.G.Clarkson, V.Hnizdo, R.J.Keddy, D.W.Mingay, F. Osterfeld and J.P.F.Sellschop - Nucl.Phys. A273, 523 (1976).
- 28) J.Shimizu, W.Yokota, T.Nakagawa, Y.Fukuchi, Y.Yamaguchi, M.Sato, S.Hanashima, Y.Nagashima, K.Furuno, K.Katori and S.Kubono - Phys.Lett. 112B, 323 (1982).

TABLE 1 - Optical potential parameters used for the calculation of the angular distributions presented in figures 6 and 7 .

POT.	V (MeV)	r_R (fm)	a_R (fm)	W (MeV)	r_I (fm)	a_I (fm)	r_C (fm)
X3	10.00	1.350	0.618	23.400	1.277	0.435	1.20
I	10.16	1.460	0.470	4.210	1.530	0.200	1.46

FIGURE CAPTIONS

FIG.1 - A typical spectrum of ^{12}C ions elastically scattered to $\theta_{\text{lab}}=40^\circ$.

FIG.2 - Spectra of ^{16}O ions provenient from the $^{24}\text{Mg}(^{12}\text{C},^{16}\text{O})^{20}\text{Ne}$ g.s. transfer reaction and from the elastic recoil of $^{16}\text{O} + ^{12}\text{C}$.

FIG.3 - Angular distribution of the elastic scattering $^{24}\text{Mg}(^{12}\text{C},^{12}\text{C})^{24}\text{Mg}$ measured at $E_{\text{LAB}}=40$ MeV.

FIG.4 - Angular distribution for the transfer reaction $^{24}\text{Mg}(^{12}\text{C},^{16}\text{O})^{20}\text{Ne}$ gs measured at $E_{\text{LAB}}=40$ MeV.

FIG.5 - The coupling scheme used in the calculations described in the text.

FIG.6 - Elastic scattering angular distributions⁽²⁶⁾ and optical potential calculations performed with potentials X3 and I (see table I) to fit the forward angle data.

FIG.7 - Elastic scattering angular distributions of Mermaz⁽¹⁰⁾ and our data, with optical model calculations that fit the forward angle data.

FIG.8 - The reflection functions of the potentials X3 and I (see table I) together with the dot-dashed line adopted as the unperturbed reflection function $|\hat{S}(\lambda)|$, with parameters $\Lambda=18.7$, $\Delta=1.3$, $\alpha=0.5$.

FIG.9 - The experimental angular distribution of the elastic

scattering, together with the elastic scattering cross-section calculated from $f(\theta)$ (unperturbed elastic scattering amplitude) as the dashed line, and the cross-section calculated taking into account the coupling to the α -transfer channel, with a phase $\phi=2.0$ between the amplitudes $f(\theta)$ and $\bar{f}(\theta)$ as the continuous line.

FIG.10 - The α -transfer reaction $^{24}\text{Mg}(^{12}\text{C},^{16}\text{O})^{20}\text{Ne}$ gs. together with the calculation in Frahn's formalism.

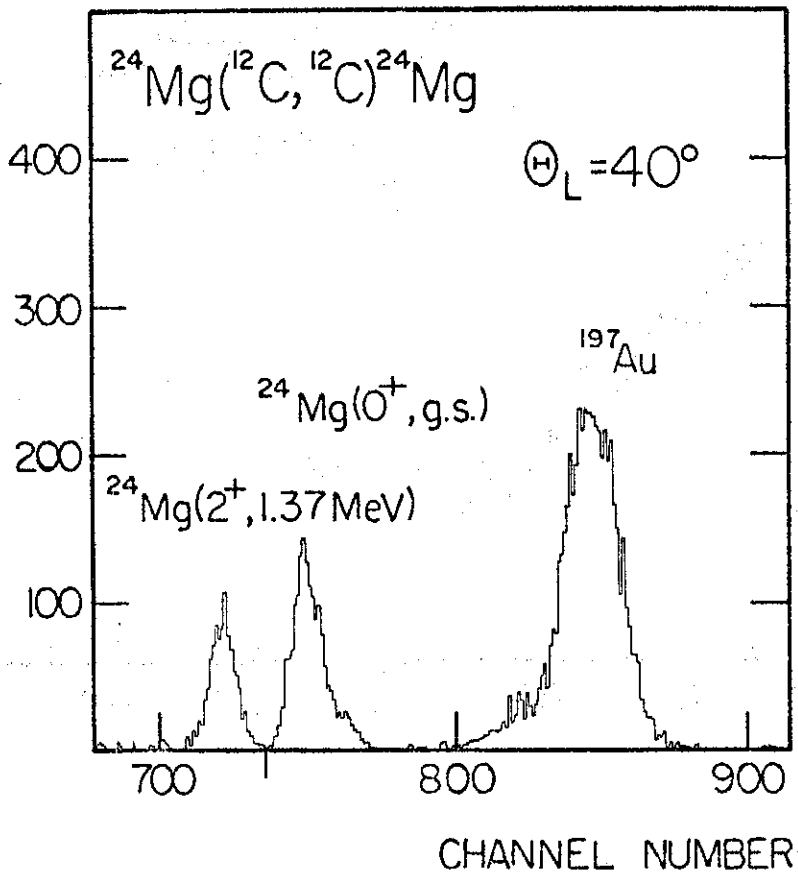


FIG. 1

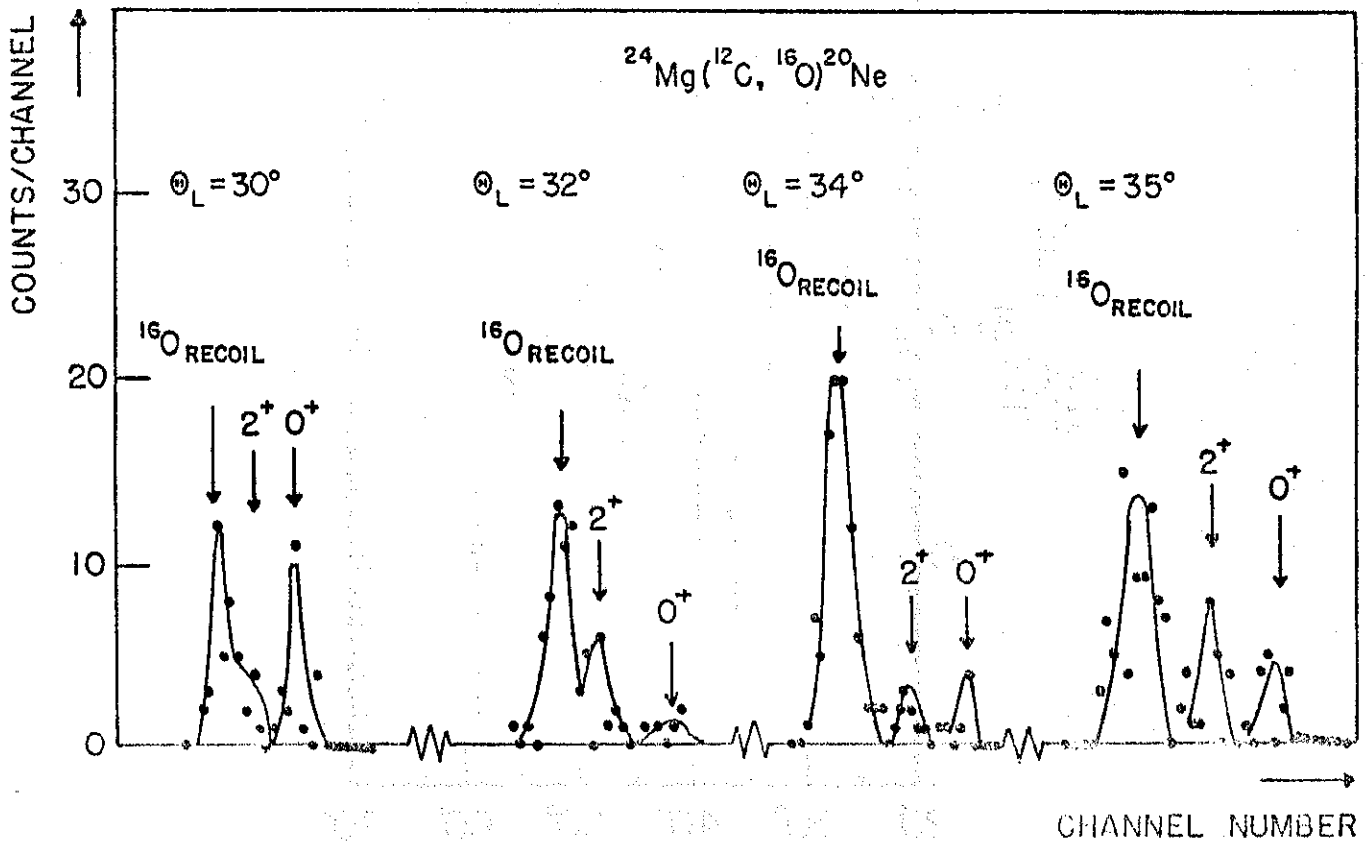


FIG. 2

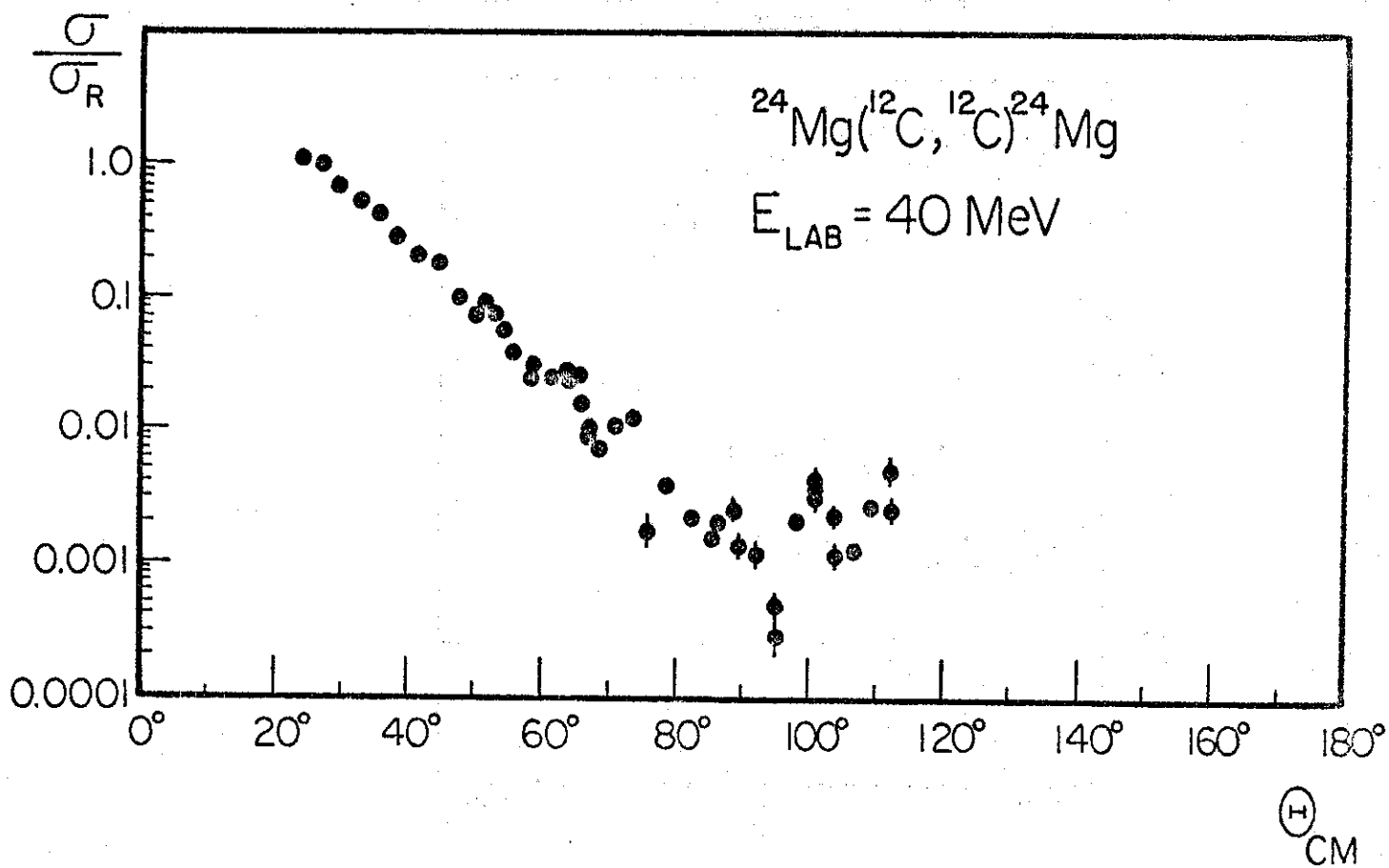


FIG. 3

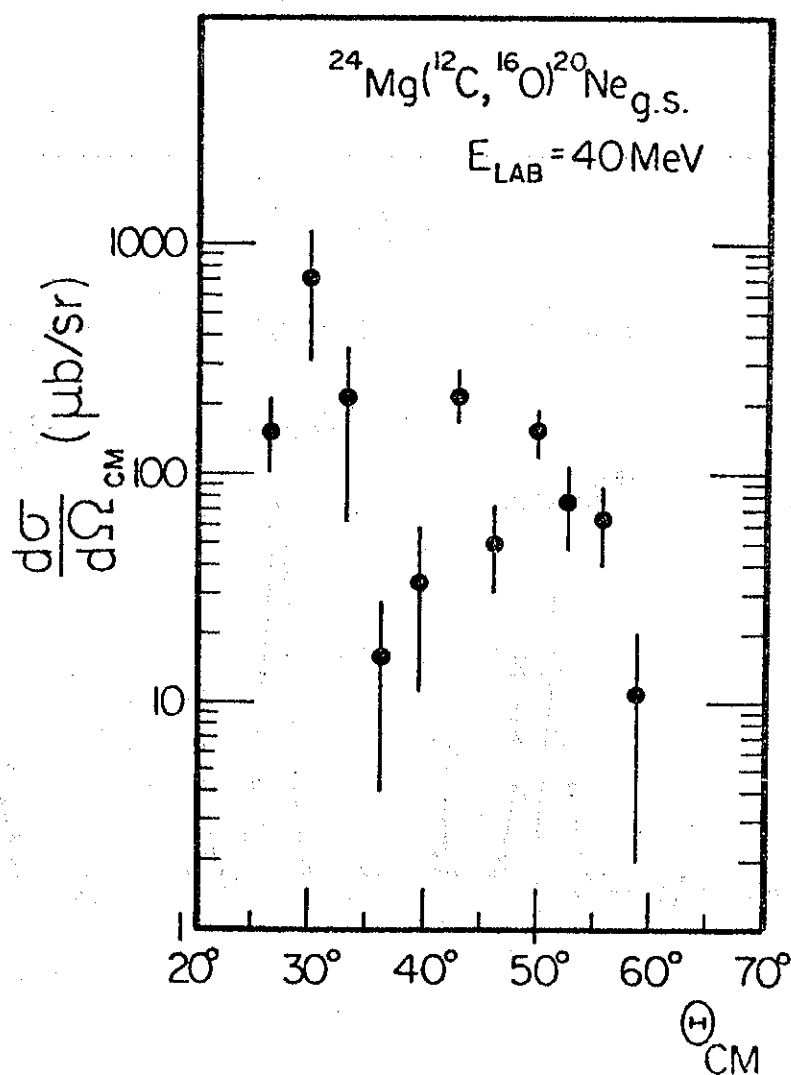


FIG. 4

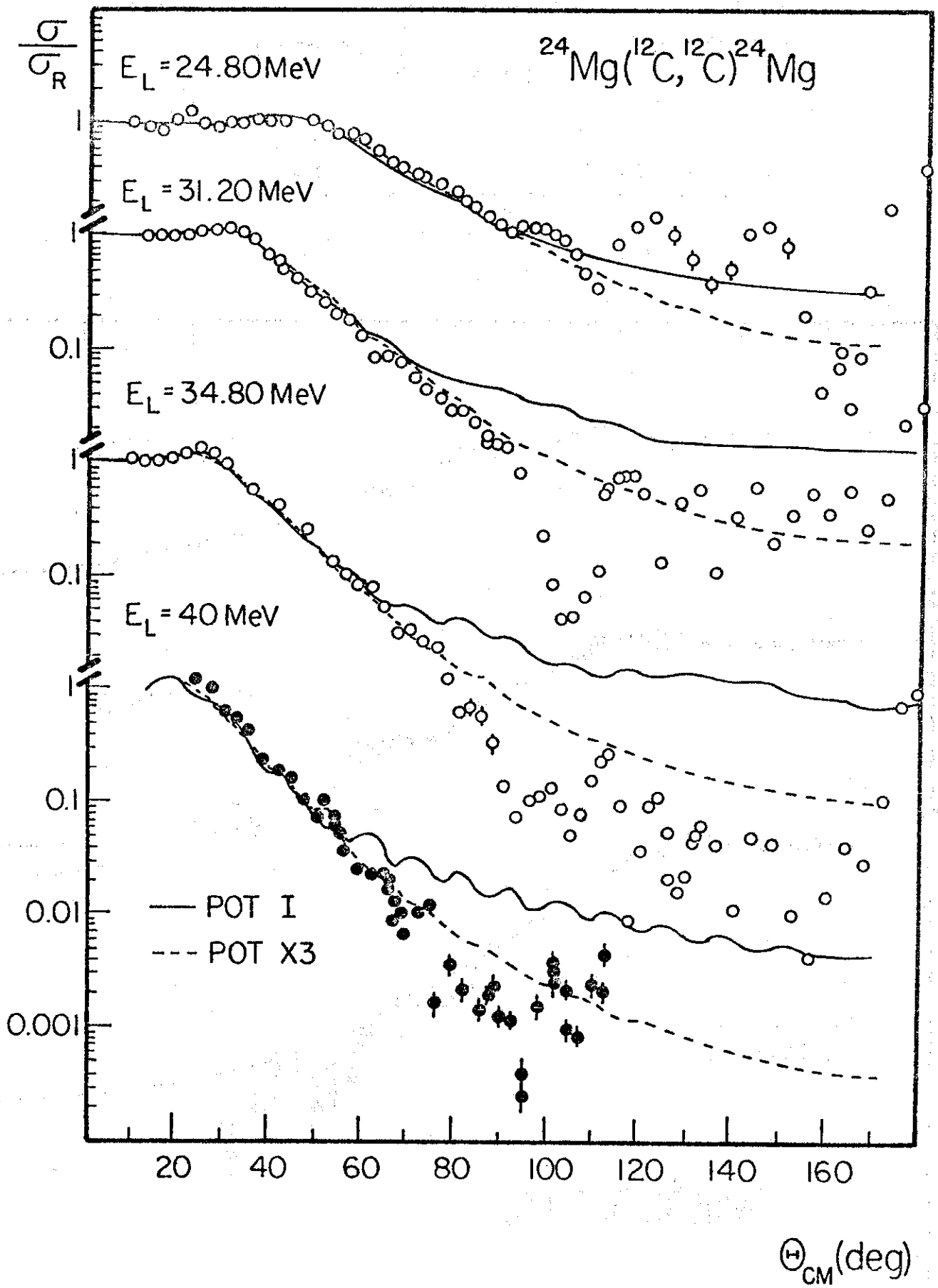


FIG. 7

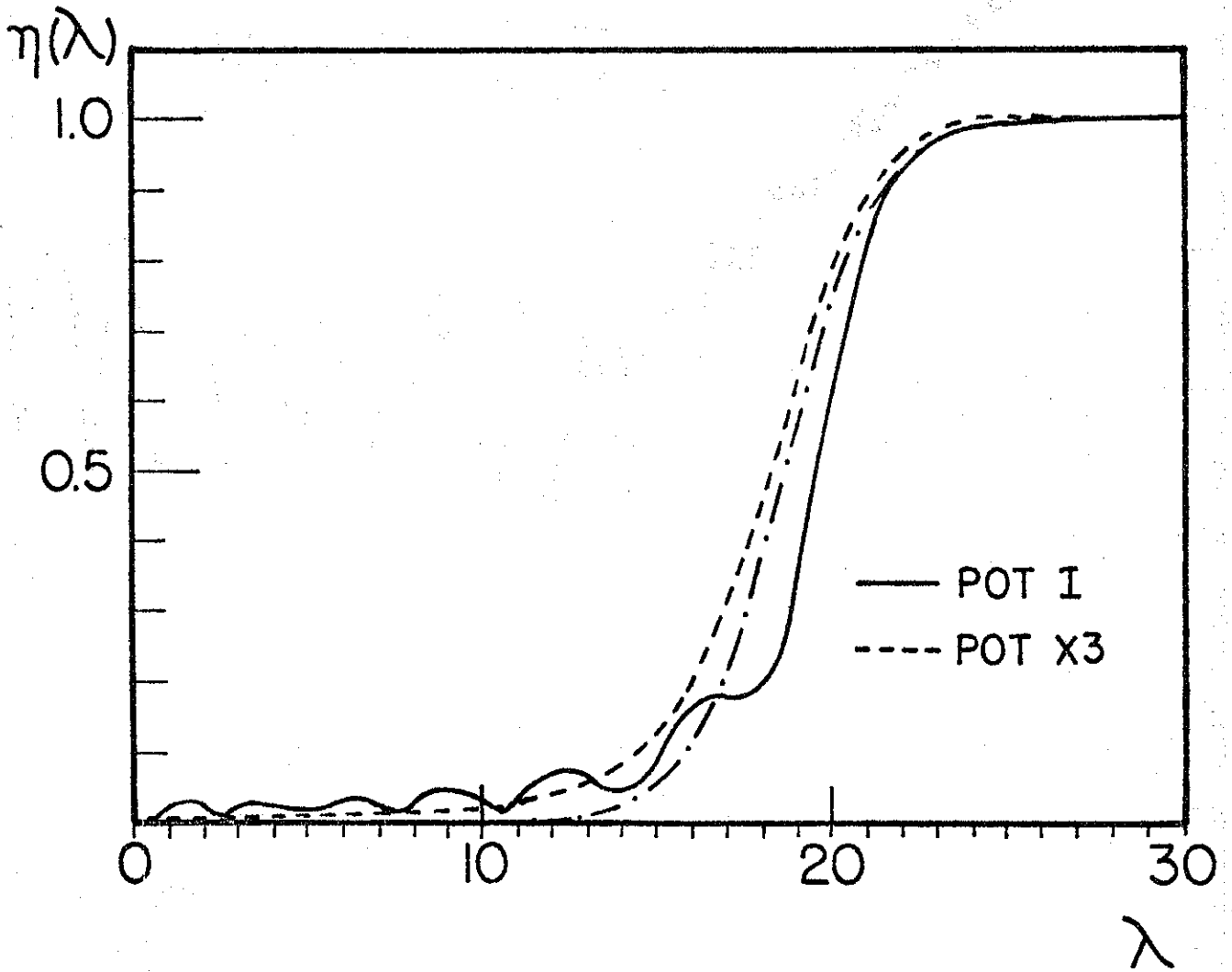


FIG. 8

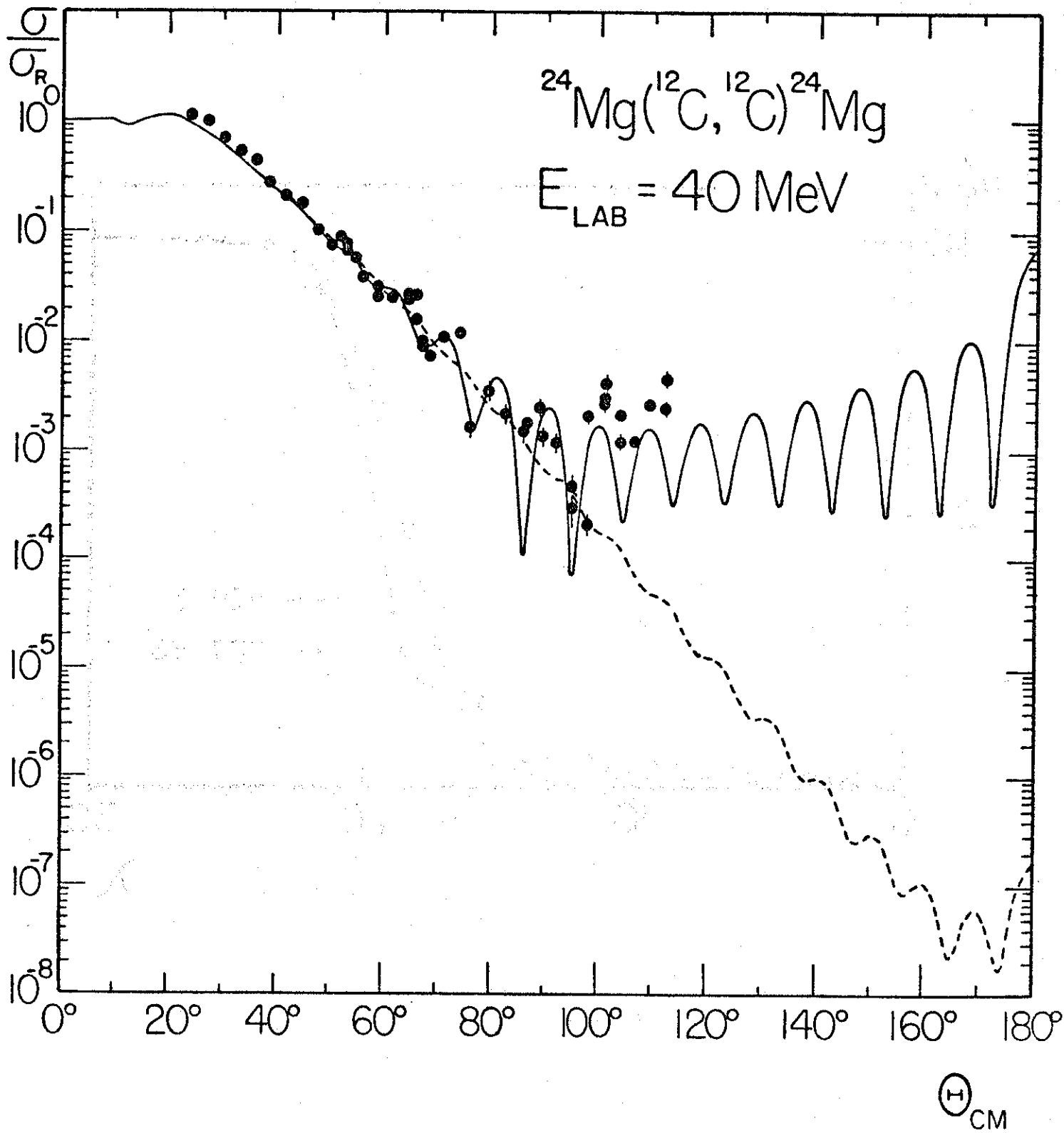


FIG. 9

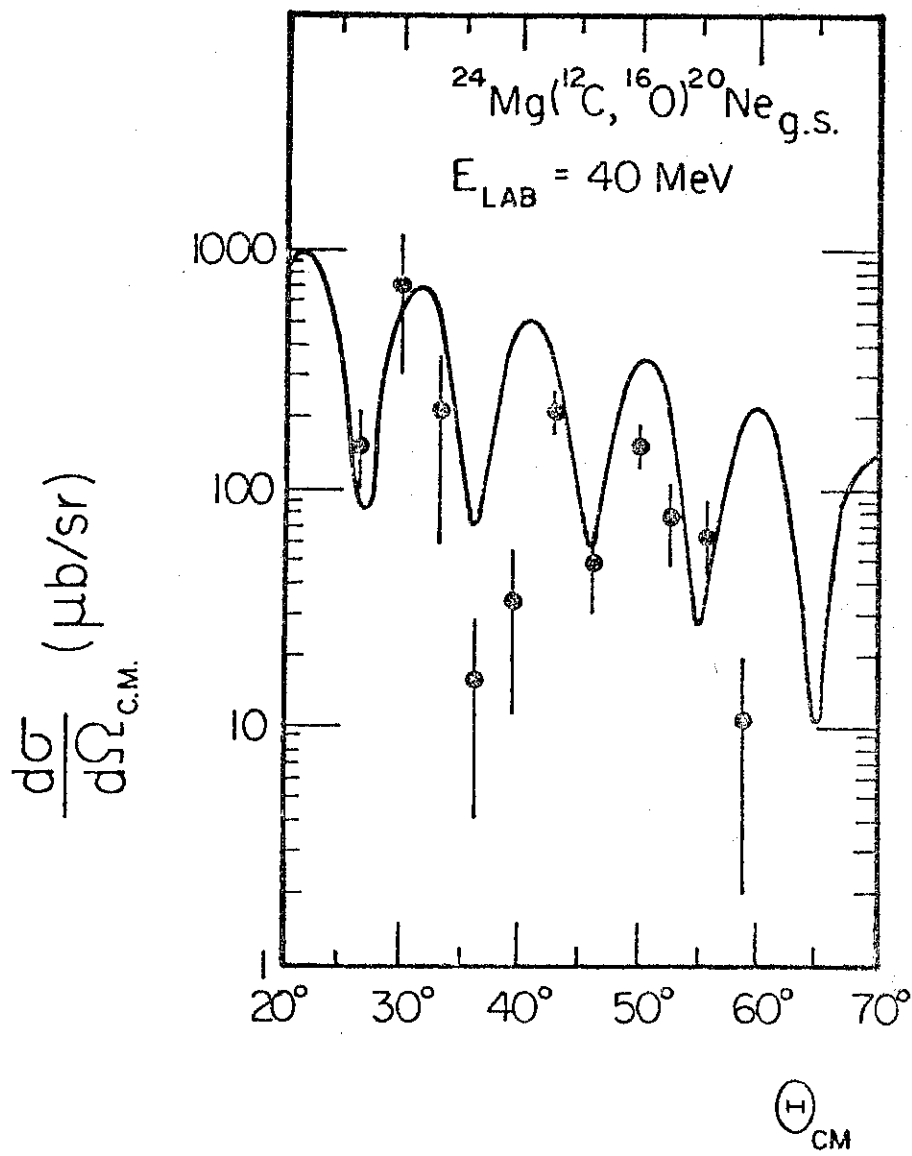


FIG. 10